Letter

Accurate and thermodynamically consistent hydrogen equation of state for planetary modeling with flow matching

Hao Xie,* Saburo Howard, and Guglielmo Mazzola†
Department of Astrophysics, University of Zürich, Winterthurerstrasse 190, 8057 Zürich, Switzerland

(Received 25 November 2024; accepted 12 July 2025; published 7 August 2025)

Accurate determination of the equation of state of dense hydrogen is essential for understanding gas giants. Currently, there is still no consensus on methods for calculating its entropy, which play a fundamental role and can result in qualitatively different predictions for Jupiter's interior. Here, we investigate various aspects of entropy calculation for dense hydrogen based on *ab initio* molecular dynamics simulations. Specifically, we employ the recently developed flow matching method to validate the accuracy of the traditional thermodynamic integration approach. We then clearly identify pitfalls in previous attempts and propose a reliable framework for constructing the hydrogen equation of state, which is accurate and thermodynamically consistent across a wide range of temperature and pressure conditions. This allows us to conclusively address the long-standing discrepancies in Jupiter's adiabat among earlier studies, demonstrating the potential of our approach for providing reliable equations of state of diverse materials.

DOI: 10.1103/n1jt-r2rj

Introduction. The equation of state (EOS) of dense hydrogen (H) is one of the core ingredients to model the internal structure of giant gaseous planets, such as Jupiter and Saturn [1]. With the wealth of data from recent spacecraft missions, *Galileo* [2] and *Juno* [3], which measured Jupiter's atmospheric composition and gravitational field, the lack of accurate knowledge of the thermodynamic properties of hydrogen is now considered as one of the major roadblocks in planetary science [4–7]. As parameterized planetary models already require several hypotheses [5,8–10], an uncontested EOS is needed to advance the field.

Since high-pressure experiments are difficult to perform and still cannot yield precise results, one usually relies instead on numerical simulations, typically *ab initio* molecular dynamics (MD) based on electron structure methods, such as density functional theory (DFT) or quantum Monte Carlo (QMC). Up to now, there have been several widely used *ab initio* EOSs for planetary science applications, including the one by Chabrier, Mazevet, and Soubiran (CMS19) [11], by Militzer and Hubbard (MH13) [12], and the Rostock EOS (REOS2 [13] and REOS3 [14]) of various versions. All of them are derived from DFT-MD simulations using the exchange-correlation functional of Perdew, Burke, and Ernzerhof (PBE) [15]. Despite this common origin, however, they can make significant differences in the resulting Jupiter model, such as the location of adiabat and the predicted size of core mass [4,7].

*Contact author: qwexiehao@gmail.com
†Contact author: guglielmo.mazzola@uzh.ch

The key factor behind these discrepancies of planetary models is the calculation of entropy, which has been recognized and discussed to some extent in several studies [4,6,12]. Unlike observables such as energy E and pressure p, the Helmholtz free energy F and entropy $S = (E - F)/T$ are not directly accessible from *ab initio* simulations and often rely on extra procedures called thermodynamic integration (TI). One common implementation of this technique involves interpolating the available data to create a continuous path on the temperature-density phase diagram [4,13]. From basic statistical mechanics, we have

$$\left(\frac{\partial}{\partial T}\frac{F}{T}\right)_{\rho} = -\frac{E}{T^2}, \quad \left(\frac{\partial}{\partial \rho}\frac{F}{T}\right)_{T} = \frac{p}{\rho^2 T}. \tag{1}$$

These two equations correspond to integrating the energy (pressure) of the system along isochores (isotherms), respectively. However, this approach has been criticized [12] because, due to the limited number of MD simulation points and inevitable statistical uncertainties in practice, the interpolation procedure may introduce systematic errors that are difficult to detect.

An alternative TI scheme is called the coupling constant integration (CCI) [16,17] or Hamiltonian thermodynamic integration [18]. By connecting the target state to an artificial Hamiltonian with known thermodynamic properties, this method further allows for the calculation of *absolute* entropy. However, it is also much more expensive due to the need to perform additional MD simulations and therefore only suitable for investigating a small region of the phase diagram [12,19]. Besides, one has to carefully choose relevant parameters in the artificial system and MD simulations to ensure well-converged results [20], and the errors associated with discreteness and statistical fluctuation of the simulation points still remain.

The uncertainties involved in entropy calculation are further exacerbated by the fact that the EOS used for planetary

modeling is usually composed of several parts, each based on different theoretical approach and has different phase region of validity. For example, although DFT-MD can provide a good description of electron correlations at intermediate temperatures and densities, especially near pressure-induced dissociation, it will quickly become inefficient at lower densities $\rho \lesssim 0.2\,\mathrm{g/cm^3}$. For such a region deep within the molecular phase, empirical chemical models, such as the well-known Saumon–Chabrier–van Horn (SCvH) EOS [21], are generally believed to be accurate and reliable. In practice, the data from these different methods need to be connected in some way. This, however, could possibly introduce critical errors, as we will demonstrate below.

In this Letter, we focus on the crucial issues of entropy calculation outlined above at the DFT-PBE level of theory, aiming to resolve long-standing disagreements among various Jupiter model predictions, which are highly sensitive to small changes in entropy [4,6,12,22]. The work is structured as follows: First, we calculate the free energy and entropy in the DFT-MD region using a recently developed method called *flow matching* [23–25]. As discussed below, such an independent approach is highly desired to benchmark the accuracy of TI and identify crucial deficiencies in previous works. Second, (and more importantly,) we devise a simple and efficient protocol to construct an EOS that can achieve excellent thermodynamic consistency *across various theories* and a broad range of conditions. Our procedure is primarily designed to provide a reliable and uncontested input for planetary modeling, thereby forming a solid foundation for future model refinements against spacecraft measurements and further applicability to other materials [1,5].

Flow matching. Consider any two given phase points (T_0, ρ_0) and (T_1, ρ_1) of the hydrogen system. When calculating their free energy difference using TI, one needs to create a continuous path between them by interpolation. On the other hand, flow matching is built on the framework of targeted free energy perturbation (TFEP) [26,27], which solely relies on information about the two end states 0 and 1; see Eqs. (2) and (3). As a result, it can avoid any errors arising from a manual interpolation procedure and thus serves as a valuable benchmark for TI.

More specifically, within the framework of TFEP, the free energy difference (scaled by temperature) between the two states can be written as the following estimators:

$$\beta_1 F_1 - \beta_0 F_0 = -\ln \mathop{\mathbb{E}}_{\boldsymbol{x}\sim p_0(\boldsymbol{x})} [e^{-\Phi_\rightarrow(\boldsymbol{x})}] = \ln \mathop{\mathbb{E}}_{\boldsymbol{x}\sim p_1(\boldsymbol{x})} [e^{\Phi_\leftarrow(\boldsymbol{x})}]. \tag{2}$$

Here, $\boldsymbol{x} \equiv (\boldsymbol{r}_1, \ldots, \boldsymbol{r}_N)$ denotes a configuration sample of the N proton coordinates, and $p_i(\boldsymbol{x}) \propto e^{-\beta_i E_i(\boldsymbol{x})}$ $(i = 0, 1)$ are the corresponding Boltzmann distributions, with $\beta_i = 1/k_B T_i$, k_B being the Boltzmann constant. The quantities

$$\Phi_\rightarrow(\boldsymbol{x}) = \beta_1 E_1(f(\boldsymbol{x})) - \beta_0 E_0(\boldsymbol{x}) - \ln \left| \det \left(\frac{\partial f(\boldsymbol{x})}{\partial \boldsymbol{x}} \right) \right|, \tag{3a}$$

$$\Phi_\leftarrow(\boldsymbol{x}) = \beta_1 E_1(\boldsymbol{x}) - \beta_0 E_0(f^{-1}(\boldsymbol{x})) + \ln \left| \det \left(\frac{\partial f^{-1}(\boldsymbol{x})}{\partial \boldsymbol{x}} \right) \right| \tag{3b}$$

are known as the *forward* and *reverse* work, respectively [28]. Note that the above equations hold in principle for *any* *invertible transformation* f that acts on the configuration space. In particular, when f is the identity map, Eqs. (2) and (3) reduce to the usual formulas for importance sampling. Moreover, we note that by simply selecting one of the states to have known thermodynamic properties, it is also fairly straightforward to compute the *absolute* free energy and entropy of the system.

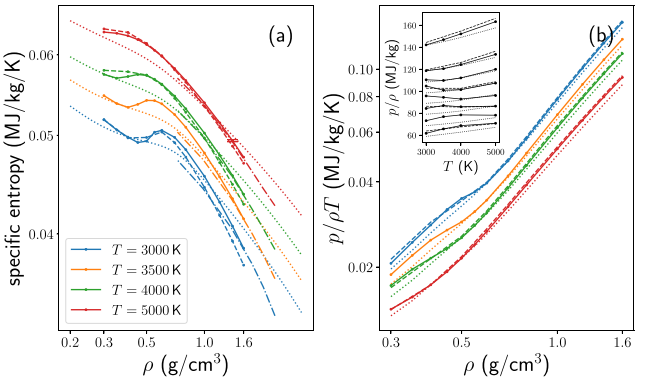

FIG. 1. (a) Specific entropy s and (b) pressure p (scaled by ρT) as a function of density ρ for several isotherms. Solid line: the present work using the flow matching method; dotted line: CMS19 [11]; dashed line: REOS3 [14]; dash-dotted line: the entropy reported by Morales *et al.* [19] based on CEIMC simulations. Note that the REOS3 entropy has been globally *shifted* to align with our results; see text for details. The inset of (b) presents the same pressure data by selected isochores, with density ranging from 0.3 (bottom) to $0.7\,\mathrm{g/cm^3}$ (top).

In practice, due to the limited number of samples, Eq. (2) can be efficiently estimated with low variance only for some carefully designed transformation f, which should bring the two states of interest close enough to ensure sufficient overlap of their probability densities. In this work, we achieve this goal by representing f as a class of generative neural network called normalizing flow [29] and training the network using the flow matching technique [23–25]. Note that, unlike the demonstrative example shown in Ref. [30], here the calculations are based on DFT-MD simulations and thus have *ab initio* accuracy. A more detailed introduction to the relevant background is provided in the Supplemental Material [28].

Entropy from ab initio data. We employ the flow matching method to study the *ab initio* portion of the phase diagram with $3000 \leqslant T \leqslant 8000\,\mathrm{K}$ and $0.3 \leqslant \rho \leqslant 1.6\,\mathrm{g/cm^3}$. Specifically, we repeatedly train a transformation f and use Eq. (2) to compute the entropy difference for each neighboring pair of states on a (T, ρ) grid; see Supplemental Material [28] for an example. We also calculate the *absolute* entropy of a reference state within the same framework and then shift the entropy of other states rigidly. In practice, we choose the reference point at $T = 5000\,\mathrm{K}$ and $\rho = 1.4\,\mathrm{g/cm^3}$ [28], where the computed value 0.0494(1) MJ/kg/K of the absolute entropy is in excellent agreement with those reported by Morales *et al.* [19] based on coupled electron-ion Monte Carlo (CEIMC) simulations.

Figure 1 shows our results (solid line) for several isotherms of the specific entropy s and pressure p, together with two widely used hydrogen EOSs in past literature: CMS19 [11]

(dotted line) and REOS3 [14] (dashed line). For convenience, we also include an error bar of absolute entropy at the reference point and the CEIMC entropy of Morales *et al.* [19] (dash-dotted line) at relatively high densities. Note that the REOS3 entropy is calculated by us using TI (see Eq. (1)), and, for the sake of visualization, we have introduced a global entropy offset to make it match our data at the bottom-left phase point, i.e., $T = 3000\,\mathrm{K}$ and $\rho = 0.3\,\mathrm{g/cm^3}$. We do not compare with the MH13 EOS since it was derived directly for a hydrogen-helium mixture, rather than the pure hydrogen system studied here.

One striking feature of Fig. 1(a) is the nonmonotonic behavior of entropy at low temperatures in both our results and REOS3, which is qualitatively different from CMS19. Moreover, CMS19 does not feature the typical slope change of the p-ρ relation, as shown in Fig. 1(b), which is emanating from the critical point of the liquid-liquid phase transition between molecular and atomic phases [31,32]. This indicates that although derived from DFT-PBE data in the phase region considered here [11,19,33,34], the CMS19 EOS does not closely capture the pressure-induced molecular dissociation, which could have a notable impact on Jupiter models [28].

According to the thermodynamic relation [21] $(\partial s/\partial \rho)_T = -\rho^{-2}(\partial p/\partial T)_\rho$, the region of "abnormally" *increasing* entropy in Fig. 1(a) corresponds precisely to that of *decreasing* pressure with temperature, as illustrated by the *isochores* in the inset of Fig. 1(b). Physically, they are just different manifestations of the molecular dissociation effects: The attractive force from broken molecular bonds can dominate the repulsion from kinetic motion, while the larger number of configurations involving only individual H atoms (compared to those with bound H_2-like pairs) can compensate for the smaller occupied volume caused by increasing density.

Benchmarking thermodynamic integration. We use the flow matching entropy in the *ab initio* region to benchmark the TI approach, which simply amounts to integrating Eq. (1) using our pressure and energy data. We find that the TI entropies are virtually indistinguishable from the solid lines in Fig. 1(a). Besides, they do not depend on the choice of integration path and hence show very good thermodynamic consistency. Our observations indicate that TI performs quite well for a discrete grid with spacings on the order of 1000 K and $0.1\,\mathrm{g/cm^3}$. When combined with the absolute entropy calculation on only a *single* reference point, as done above, we can then achieve the same level of accuracy as the "full" CCI approach in Ref. [12] but with far less computational costs.

Note that, compared to REOS3, we have selected a slightly denser grid of simulation points between 0.3 and $0.6\,\mathrm{g/cm^3}$ to improve the characterization of molecular dissociation. Nevertheless, the "discreteness" error of TI in the *ab initio* region of REOS3 is still under control, and the resulting entropy remains generally consistent with our data, as shown by the dashed lines in Fig. 1(a). However, TI becomes truly problematic when we further extend the integration path to touch other regions based on inconsistent theories. We can quantitatively illustrate such inconsistency by performing the line integral $\oint d(F/T)$ along each closed local square loop of the tabular data, which should, in principle, vanish everywhere. However, for REOS3, we found large deviation from this ideal behavior between the *ab initio* region and the chemical model at lower densities [35,36], as shown in Fig. 2. This implies that the resulting entropy will be *ambiguously* defined and strongly depend on the choice of integration path and initial reference point; see Supplemental Material [28] for more details. One can then identify an entropy error of approximately 10% [28], which yields qualitatively large differences on planetary models derived in the past using this method [4,13].

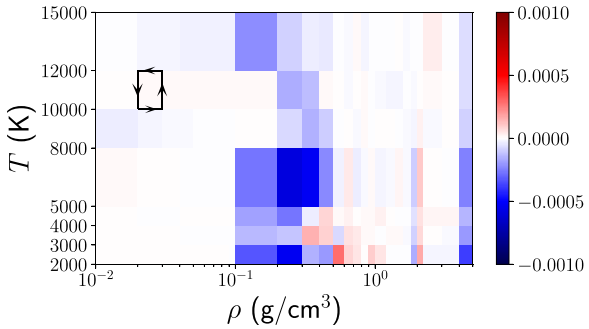

FIG. 2. The line integral $\oint d(F/T)$ (in units of MJ/kg/K) computed along each closed local square loop of the REOS3 data. A schematic example of the loop is shown on the top-left corner.

Thermodynamically consistent construction. An inherent difficulty of the "single TI over the entire phase diagram" approach stems from the fact that energy and pressure are different partial derivatives of the same free energy function and hence *not independent*. Consequently, it turns out to be highly challenging to simultaneously interpolate *both* energy and pressure data produced by different theories *in a consistent way*, as demonstrated in Fig. 2 for the case of REOS3. A better approach is to perform TI on each component (i.e., region where the same theory applies) of the EOS *separately* and then interpolate the resulting *free energy* function [28]. In this way, one can derive the pressure and energy near the interpolation boundaries by taking partial derivatives, which are naturally consistent by construction. Another advantage is that one can easily incorporate accurate values of the *absolute* entropy into each separate region. This ensures that any residual interpolation errors that one can make at the boundaries remain localized and do not propagate elsewhere.

Figures 3(a)–3(d) show our final EOS (solid lines), which consists of the *ab initio* DFT-MD part at $\rho \geqslant 0.3\,\mathrm{g/cm^3}$ (only above 3000 K), the SCvH EOS at $\rho \leqslant 0.1\,\mathrm{g/cm^3}$ (covering a broader temperature range down to ∼100 K), and an interpolation region between them. For comparison, we also include the entropy and pressure isotherms of Miguel *et al.* [4] (dashed lines), which are obtained by a single TI over the entire phase region of REOS3. Note that the new interpolation procedure depends very sensitively on the entropy difference between SCvH and the *ab initio* data [28]. In particular, a high-quality interpolation can only be achieved after globally subtracting a constant of 0.0057 MJ/kg/K from the originally reported SCvH entropy. Remarkably, this observation aligns precisely with various independent numerical [11] and experimental references [37,38]. There, the entropy constant was recognized as $k_B \ln 2/m_\mathrm{p}$, which accounts for the contribution of proton spin degrees of freedom that are implicitly neglected on the DFT-MD side [39]; see Supplemental Material [28] for details. This strongly indicates that our new protocol is indeed

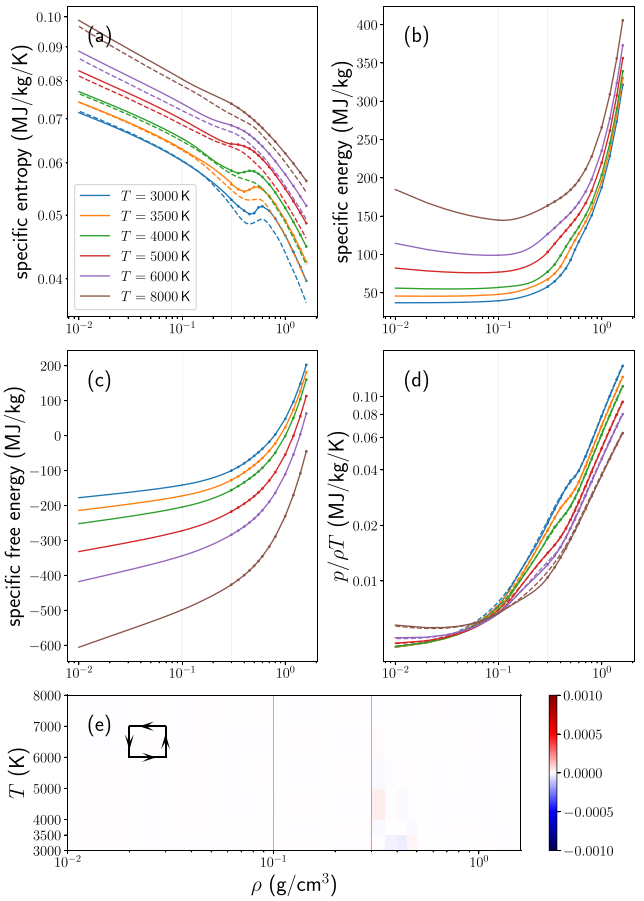

FIG. 3. Several (a) specific entropy, (b) specific energy, (c) specific free energy, and (d) pressure (scaled by ρT) isotherms of our final EOS (solid lines), which consist of the *ab initio* data at high densities, the SCvH EOS at low densities, and an interpolation region between them, as indicated by the vertical lines. The dashed lines are the entropy and pressure isotherms of Miguel *et al.* [4], obtained by performing a single TI over the entire phase region of REOS3. Note that we have added an extra entropy shift of -0.0057 MJ/kg/K to both the dashed lines and SCvH part of the solid lines in panel (a); see text for details. Panel (e) shows the local loop integral values $\oint d(F/T)$ of our EOS, similar to Fig. 2 for the case of REOS3.

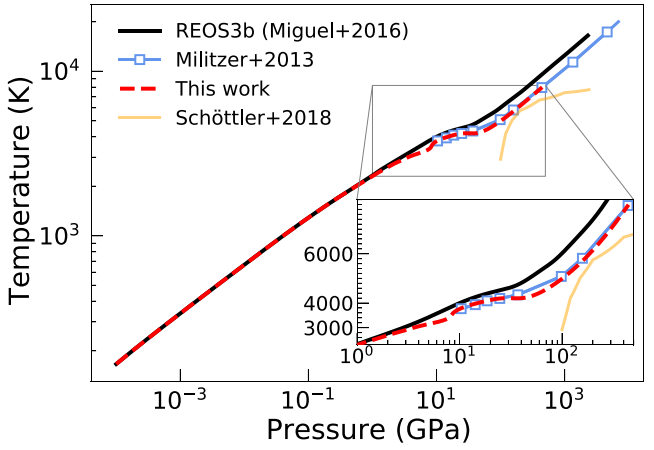

FIG. 4. Jupiter's adiabats obtained from different EOSs. See text for a detailed comparison between our result (red dashed line) and those derived from the REOS3 (black line) [22] and MH13 EOS (blue line) [12]. The yellow line shows the hydrogen-helium demixing curve for a protosolar mixture from Ref. [40].

the very approach to construct accurate and uncontested hydrogen EOS for planetary modeling. Figure 3(e) also shows the local loop integral values $\oint d(F/T)$ of our final EOS; compared to Fig. 2, one clearly sees that the new protocol can indeed yield much better thermodynamic consistency over the entire phase diagram, as discussed above.

Jupiter's adiabat. We demonstrate the utility of the newly constructed hydrogen EOS by performing a preliminary calculation of Jupiter's adiabat. We assume a homogeneous model with no compact core and set a helium mass fraction of $Y = 0.245$ to ensure a fair comparison with previous works [4,12,22]. We adopt a simple linear mixing approximation for the entropy of mixtures, using the REOS3 EOS of helium derived by Miguel *et al.* in Ref. [22].

Figure 4 shows our result for the adiabat (red dashed line) together with those derived from the REOS3 (black line) [22] and MH13 EOS (blue line) [12], respectively. For a comparison also with CMS19, see the Supplemental Material [28]. Note that the hydrogen EOS used in the REOS3 adiabat was produced by Miguel *et al.* [4,22] using a single TI over the entire phase region, as already shown by the dashed lines in Fig. 3. Our result clearly agrees well with the REOS3 adiabat up to about 1 GPa, which is as expected since both the underlying hydrogen EOSs are derived at low pressures from the same SCvH model. However, at higher pressures, our adiabat begins to diverge from the REOS3 line and becomes cooler. This is a direct consequence of the systematically lower REOS3 entropy in the *ab initio* region in Fig. 3(a), which is in turn caused by the thermodynamic inconsistency shown in Fig. 2 [28]. Notice that such a cooler adiabat passes very close to the miscibility boundary for hydrogen-helium mixtures, shown by the yellow line in Fig. 4, albeit derived from DFT-MD simulations using an exchange-correlation functional different from PBE [40]. This suggests an increased likelihood of phase separation between hydrogen and helium in Jupiter's deep interior, causing the formation of so-called helium rain [1,41,42].

On the other hand, our adiabat at high pressures is apparently closer to the MH13 prediction, as shown by the blue line in Fig. 4. Note that the MH13 EOS is derived directly from *ab initio* MD simulations of a hydrogen-helium mixture and does not rely on the linear mixing approximation. Overall, we show that, at the DFT-PBE level of theory, the long-standing discrepancy between the Jupiter models of REOS3 and MH13 primarily stems from a problematic TI calculation of the REOS3 entropy that is not everywhere thermodynamically consistent. However, according to our earlier benchmark using flow matching, this definitely does *not* imply that TI is inherently inferior to the CCI approach for a finite number of simulation points, as speculated in Ref. [12]. Another observation from Fig. 4 is that the MH13 adiabat [12] was derived only for the *ab initio* region at high pressures. In fact, Ref. [12] did not really attempt a thermodynamic consistent interpolation with other regions to construct a complete EOS,

which, however, is definitely needed for a thorough study of planetary models.

Summary and outlook. In this Letter, we closely examine the entropy calculation of dense hydrogen in the *ab initio* region by benchmarking TI with an independent flow matching method. Building on this, we then construct a new hydrogen EOS that is both accurate and thermodynamically consistent over several orders of magnitude of pressure (roughly 1 bar $\sim$ 700 GPa). Remarkably, the interpolation quality at the boundaries serves as a highly sensitive and stringent "detector" for the accuracy of the theories on both sides [28]. Such a "self-correcting" mechanism of the new protocol is exactly what we need to ensure steady convergence toward a truly reliable and conclusive hydrogen EOS for planetary modeling.

We conclusively address the long-standing issue of entropy disagreements among various popular EOSs used in planetary modeling [11,12,14], all of which are derived from the same DFT-PBE level of electronic structure theory. To further improve the hydrogen EOS and potentially reconcile models with observational data [5], one can upgrade the description of electronic correlation from DFT-PBE to a higher-level theory [43–46]. We also note that, as a generic tool, flow matching can also be used to study other rich phases of hydrogen [47,48] or other interesting condensed matter systems [42,49], where accurate calculation of free energy plays a significant role.

Acknowledgments. We acknowledge useful discussions with Lei Wang, Ravit Helled, Didier Saumon, Gilles Chabrier, and Armin Bergermann. We also acknowledge Cesare Cozza for providing initial data and support with the DFT calculations. H.X. and G.M. acknowledge financial support from the Swiss National Science Foundation (Grant No. PCEFP2_-203455). S.H. also acknowledges financial support from the Swiss National Science Foundation (Grant No. 200020_-215634).

Data availability. The data that support the findings of this article are not publicly available. The data are available from the authors upon reasonable request.

[1] R. Helled, G. Mazzola, and R. Redmer, Understanding dense hydrogen at planetary conditions, Nat. Rev. Phys. **2**, 562 (2020).
[2] T. V. Johnson, C. M. Yeates, and R. Young, Space science reviews volume on Galileo Mission overview, Space Sci. Rev. **60**, 3 (1992).
[3] S. J. Bolton, J. Lunine, D. Stevenson, J. E. P. Connerney, S. Levin, T. C. Owen, F. Bagenal, D. Gautier, A. P. Ingersoll, G. S. Orton, T. Guillot, W. Hubbard, J. Bloxham, A. Coradini, S. K. Stephens, P. Mokashi, R. Thorne, and R. Thorpe, The Juno mission, Space Sci. Rev. **213**, 5 (2017).
[4] Y. Miguel, T. Guillot, and L. Fayon, Jupiter internal structure: The effect of different equations of state, Astron. Astrophys. **596**, A114 (2016).
[5] F. Debras and G. Chabrier, New models of Jupiter in the context of Juno and Galileo, Astrophys. J. **872**, 100 (2019).
[6] S. Mazevet, A. Licari, and F. Soubiran, Benchmarking the *ab initio* hydrogen equation of state for the interior structure of Jupiter, Astron. Astrophys. **664**, A112 (2022).
[7] S. Howard, T. Guillot, M. Bazot, Y. Miguel, D. J. Stevenson, E. Galanti, Y. Kaspi, W. B. Hubbard, B. Militzer, R. Helled, N. Nettelmann, B. Idini, and S. Bolton, Jupiter's interior from Juno: Equation-of-state uncertainties and dilute core extent, Astron. Astrophys. **672**, A33 (2023).
[8] N. Nettelmann, N. Movshovitz, D. Ni, J. J. Fortney, E. Galanti, Y. Kaspi, R. Helled, C. R. Mankovich, and S. Bolton, Theory of figures to the seventh order and the interiors of Jupiter and Saturn, Planet. Sci. J. **2**, 241 (2021).
[9] Y. Miguel, M. Bazot, T. Guillot, S. Howard, E. Galanti, Y. Kaspi, W. B. Hubbard, B. Militzer, R. Helled, S. K. Atreya, J. E. P. Connerney, D. Durante, L. Kulowski, J. I. Lunine, D. Stevenson, and S. Bolton, Jupiter's inhomogeneous envelope, Astron. Astrophys. **662**, A18 (2022).
[10] B. Militzer, W. B. Hubbard, S. Wahl, J. I. Lunine, E. Galanti, Y. Kaspi, Y. Miguel, T. Guillot, K. M. Moore, M. Parisi, J. E. P. Connerney, R. Helled, H. Cao, C. Mankovich, D. J. Stevenson, R. S. Park, M. Wong, S. K. Atreya, J. Anderson, and S. J. Bolton, Juno spacecraft measurements of Jupiter's gravity imply a dilute core, Planet. Sci. J. **3**, 185 (2022).
[11] G. Chabrier, S. Mazevet, and F. Soubiran, A new equation of state for dense hydrogen–helium mixtures, Astrophys. J. **872**, 51 (2019).
[12] B. Militzer and W. B. Hubbard, *Ab initio* equation of state for hydrogen–helium mixtures with recalibration of the giant-planet mass–radius relation, Astrophys. J. **774**, 148 (2013).
[13] N. Nettelmann, A. Becker, B. Holst, and R. Redmer, Jupiter models with improved *ab initio* hydrogen equation of state (H-REOS.2), Astrophys. J. **750**, 52 (2012).
[14] A. Becker, W. Lorenzen, J. J. Fortney, N. Nettelmann, M. Schöttler, and R. Redmer, *Ab initio* equations of state for hydrogen (H-REOS.3) and helium (He-REOS.3) and their implications for the interior of brown dwarfs, Astrophys. J. Suppl. Ser. **215**, 21 (2014).
[15] J. P. Perdew, K. Burke, and M. Ernzerhof, Generalized gradient approximation made simple, Phys. Rev. Lett. **77**, 3865 (1996).
[16] J. G. Kirkwood, Statistical mechanics of fluid mixtures, J. Chem. Phys. **3**, 300 (1935).
[17] G. A. de Wijs, G. Kresse, and M. J. Gillan, First-order phase transitions by first-principles free-energy calculations: The melting of Al, Phys. Rev. B **57**, 8223 (1998).
[18] D. Frenkel and B. Smit, *Understanding Molecular Simulation: From Algorithms to Applications*, 3rd ed. (Academic Press, Cambridge, Massachusetts, USA, 2023).
[19] M. A. Morales, C. Pierleoni, and D. M. Ceperley, Equation of state of metallic hydrogen from coupled electron-ion Monte Carlo simulations, Phys. Rev. E **81**, 021202 (2010).
[20] A. Bergermann, M. French, and R. Redmer, *Ab initio* calculation of the miscibility diagram for mixtures of hydrogen and water, Phys. Rev. B **109**, 174107 (2024).
[21] D. Saumon, G. Chabrier, and H. M. van Horn, An equation of state for low-mass stars and giant planets, Astrophys. J. Suppl. Ser. **99**, 713 (1995).
[22] Y. Miguel, T. Guillot, and L. Fayon, Jupiter internal structure: The effect of different equations of state (corrigendum), Astron. Astrophys. **618**, C2 (2018).

[23] M. S. Albergo and E. Vanden-Eijnden, Building normalizing flows with stochastic interpolants, in *The Eleventh International Conference on Learning Representations* (2023).

[24] Y. Lipman, R. T. Q. Chen, H. Ben-Hamu, M. Nickel, and M. Le, Flow matching for generative modeling, in *The Eleventh International Conference on Learning Representations* (2023).

[25] X. Liu, C. Gong, and Qiang Liu, Flow straight and fast: Learning to generate and transfer data with rectified flow, in *The Eleventh International Conference on Learning Representations* (2023).

[26] C. Jarzynski, Targeted free energy perturbation, Phys. Rev. E **65**, 046122 (2002).

[27] A. M. Hahn and H. Then, Using bijective maps to improve free-energy estimates, Phys. Rev. E **79**, 011113 (2009).

[28] See Supplemental Material at http://link.aps.org/supplemental/10.1103/n1jt-r2rj for more details on the theoretical formulations of targeted free energy perturbation and flow matching, as well as their implementation and some illustrative examples in practice. There are also further discussions about the effects of thermodynamic inconsistency on entropy calculation, our new EOS construction approach, and the comparison between Jupiter's adiabats derived from various hydrogen EOSs.

[29] G. Papamakarios, E. Nalisnick, D. J. Rezende, S. Mohamed, and B. Lakshminarayanan, Normalizing flows for probabilistic modeling and inference, J. Mach. Learn. Res. **22**, 1 (2021).

[30] L. Zhao and L. Wang, Bounding free energy difference with flow matching, Chin. Phys. Lett. **40**, 120201 (2023).

[31] W. Lorenzen, B. Holst, and R. Redmer, First-order liquid-liquid phase transition in dense hydrogen, Phys. Rev. B **82**, 195107 (2010).

[32] H. Y. Geng, Q. Wu, M. Marqués, and G. J. Ackland, Thermodynamic anomalies and three distinct liquid-liquid transitions in warm dense liquid hydrogen, Phys. Rev. B **100**, 134109 (2019).

[33] L. Caillabet, S. Mazevet, and P. Loubeyre, Multiphase equation of state of hydrogen from *ab initio* calculations in the range 0.2 to 5 g/cc up to 10 eV, Phys. Rev. B **83**, 094101 (2011).

[34] B. Holst, R. Redmer, and M. P. Desjarlais, Thermophysical properties of warm dense hydrogen using quantum molecular dynamics simulations, Phys. Rev. B **77**, 184201 (2008).

[35] H. Juranek, R. Redmer, and Y. Rosenfeld, Fluid variational theory for pressure dissociation in dense hydrogen: Multicomponent reference system and nonadditivity effects, J. Chem. Phys. **117**, 1768 (2002).

[36] B. Holst, N. Nettelmann, and R. Redmer, Equation of state for dense hydrogen and plasma phase transition, Contrib. Plasma Phys. **47**, 368 (2007).

[37] J. D. Cox, D. D. Wagman, and V. A. Medvedev, *CODATA key values for thermodynamics* (Hemisphere Publishing Corporation, New York, USA, 1989).

[38] E. W. Lemmon, I. H. Bell, M. L. Huber, and M. O. McLinden, Thermophysical properties of fluid systems, in *NIST Chemistry WebBook, NIST Standard Reference Database Number 69*, edited by P. J. Linstrom and W. G. Mallard (National Institute of Standards and Technology, Gaithersburg, MD, 2023).

[39] D. Saumon and G. Chabrier (private communication).

[40] M. Schöttler and R. Redmer, *Ab initio* calculation of the miscibility diagram for hydrogen-helium mixtures, Phys. Rev. Lett. **120**, 115703 (2018).

[41] J. Vorberger, I. Tamblyn, B. Militzer, and S. A. Bonev, Hydrogen-helium mixtures in the interiors of giant planets, Phys. Rev. B **75**, 024206 (2007).

[42] X. Chang, B. Chen, Q. Zeng, H. Wang, K. Chen, Q. Tong, X. Yu, D. Kang, S. Zhang, F. Guo, Y. Hou, Z. Zhao, Y. Yao, Y. Ma, and J. Dai, Theoretical evidence of H-He demixing under Jupiter and Saturn conditions, Nat. Commun. **15**, 8543 (2024).

[43] C. Pierleoni, M. A. Morales, G. Rillo, M. Holzmann, and D. M. Ceperley, Liquid–liquid phase transition in hydrogen by coupled electron–ion Monte Carlo simulations, Proc. Natl. Acad. Sci. **113**, 4953 (2016).

[44] G. Mazzola, R. Helled, and S. Sorella, Phase diagram of hydrogen and a hydrogen-helium mixture at planetary conditions by quantum Monte Carlo simulations, Phys. Rev. Lett. **120**, 025701 (2018).

[45] K. Nakano, C. Attaccalite, M. Barborini, L. Capriotti, M. Casula, E. Coccia, M. Dagrada, C. Genovese, Y. Luo, G. Mazzola, A. Zen, and S. Sorella, TurboRVB: A many-body toolkit for *ab initio* electronic simulations by quantum Monte Carlo, J. Chem. Phys. **152**, 204121 (2020).

[46] H. Xie, Z.-H. Li, H. Wang, L. Zhang, and L. Wang, Deep variational free energy approach to dense hydrogen, Phys. Rev. Lett. **131**, 126501 (2023).

[47] M. A. Morales, C. Pierleoni, E. Schwegler, and D. M. Ceperley, Evidence for a first-order liquid-liquid transition in high-pressure hydrogen from *ab initio* simulations, Proc. Natl. Acad. Sci. USA **107**, 12799 (2010).

[48] H. Niu, Y. Yang, S. Jensen, M. Holzmann, C. Pierleoni, and D. M. Ceperley, Stable solid molecular hydrogen above 900 K from a machine-learned potential trained with diffusion quantum Monte Carlo, Phys. Rev. Lett. **130**, 076102 (2023).

[49] X. Wang, Z. Wang, P. Gao, C. Zhang, J. Lv, H. Wang, H. Liu, Y. Wang, and Y. Ma, Data-driven prediction of complex crystal structures of dense lithium, Nat. Commun. **14**, 2924 (2023).